



HAL
open science

The Three-Dimensional Light Field Within Sea Ice Ridges

Christian Katlein, Jean-philippe Langelier, Alexandre Ouellet, Félix Lévesque-desrosiers, Quentin Hisette, Benjamin Lange, Simon Lambert-girard, Marcel Babin, Simon Thibault

► **To cite this version:**

Christian Katlein, Jean-philippe Langelier, Alexandre Ouellet, Félix Lévesque-desrosiers, Quentin Hisette, et al.. The Three-Dimensional Light Field Within Sea Ice Ridges. *Geophysical Research Letters*, 2021, 48 (11), 10.1029/2021GL093207. hal-03458205

HAL Id: hal-03458205

<https://hal.science/hal-03458205>

Submitted on 8 Apr 2022

HAL is a multi-disciplinary open access archive for the deposit and dissemination of scientific research documents, whether they are published or not. The documents may come from teaching and research institutions in France or abroad, or from public or private research centers.

L'archive ouverte pluridisciplinaire **HAL**, est destinée au dépôt et à la diffusion de documents scientifiques de niveau recherche, publiés ou non, émanant des établissements d'enseignement et de recherche français ou étrangers, des laboratoires publics ou privés.

Copyright

Geophysical Research Letters



RESEARCH LETTER

10.1029/2021GL093207

Key Points:

- We computed the full three-dimensional light field inside and underneath a pressure ridge
- Scalar irradiance is enhanced within the ridge compared to under level ice
- Simple parameterizations can capture key aspects of the ridge light field, for example, for habitat characterization and large scale models

Correspondence to:

C. Katlein,
Christian.Katlein@awi.de

Citation:

Katlein, C., Langelier, J.-P., Ouellet, A., Lévesque-Desrosiers, F., Hisette, Q., Lange, B. A., et al. (2021). The three-dimensional light field within sea ice ridges. *Geophysical Research Letters*, 48, e2021GL093207. <https://doi.org/10.1029/2021GL093207>

Received 2 MAR 2021

Accepted 14 MAY 2021

Author Contributions:

Conceptualization: Christian Katlein, Simon Lambert-Girard

Formal analysis: Christian Katlein, Jean-Philippe Langelier

Funding acquisition: Christian Katlein, Marcel Babin, Simon Thibault

Investigation: Christian Katlein, Benjamin A. Lange, Simon Lambert-Girard

Methodology: Alexandre Ouellet, Félix Lévesque-Desrosiers

Resources: Quentin Hisette

Software: Jean-Philippe Langelier, Alexandre Ouellet, Félix Lévesque-Desrosiers, Simon Thibault

Supervision: Christian Katlein, Simon Lambert-Girard, Marcel Babin, Simon Thibault

Writing – original draft: Christian Katlein

The Three-Dimensional Light Field Within Sea Ice Ridges

Christian Katlein^{1,2} , Jean-Philippe Langelier^{2,3}, Alexandre Ouellet³, Félix Lévesque-Desrosiers^{2,3} , Quentin Hisette⁴, Benjamin A. Lange⁵ , Simon Lambert-Girard² , Marcel Babin² , and Simon Thibault³ 

¹Alfred-Wegener-Institut Helmholtz Zentrum für Polar- und Meeresforschung, Bremerhaven, Germany, ²Takuvik Joint International Laboratory, Université Laval and CNRS, Québec, Canada, ³Centre d'Optique, Photonique et Laser (COPL) and Département de Physique, de Génie Physique et d'Optique, Université Laval, Québec, Canada, ⁴Hamburg Ship Model Basin (HSVA), Hamburg, Germany, ⁵Fram Centre, Norwegian Polar Institute, Tromsø, Norway

Abstract Sea ice pressure ridges have been recognized as important locations for both physical and biological processes. Thus, understanding the associated light-field is crucial, but their complex structure and internal geometry render them hard to study by field methods. To calculate the in- and under-ridge light field, we combined output from an ice mechanical model with a Monte-Carlo ray tracing simulation. This results in realistic light fields showing that light levels within the ridge itself are significantly higher than under the surrounding level ice. Light guided through ridge cavities and scattering in between ridge blocks also results in a more isotropic ridge-internal light field. While the true variability of light transmittance through a ridge can only be represented in ray tracing models, we show that simple parameterizations based on ice thickness and macro-porosity allow accurate estimation of mean light levels available for photosynthesis underneath ridges in field studies and large-scale models.

Plain Language Summary When two slabs of sea ice collide, they can break and form pressure ridges by piling up loose ice blocks over each other. The light environment within these ridges is very complicated, but also crucial for their characteristics as habitat for the sea ice ecosystem. We calculate the light field within and underneath such a pressure ridge by tracing the path of many individual photons through the ridge geometry. Our results show that light levels within the ridge can be higher than in the adjacent undeformed ice. We suggest simple equations that can be used in large scale models to estimate the light intensity underneath the pressure ridge based on ice geometry data that can be obtained in the field.

1. Introduction

Investigating the optical properties of sea ice is an important key to accurately understand the energy transfer across the atmosphere-ice-ocean boundary. Recent changes in the physical properties of the Antarctic and, more notably the Arctic sea ice cover, have resulted in increased light transmittance of the ice pack with important consequences for the physical and biological systems (Meier et al., 2014; Nicolaus et al., 2012). A large number of studies have investigated the optical properties of sea ice, but most studies focused on undeformed, level and relatively more homogeneous sea ice. While some studies include deformation features such as pressure ridges (Katlein et al., 2019; Lange, Flores, et al., 2017; Massicotte et al., 2019), there has been no dedicated investigation of the light field within and underneath these features, besides their general effect of significantly lowering light transmittance.

Sea ice pressure ridges form during periods of ice convergence, when two slabs of sea ice collide, shear, and break up into blocks that pile up above and below the water line (Davis & Wadhams, 1995; Timco & Burden, 1997). The portion above the water line is called the ridge sail and is important for snow accumulation and atmospheric turbulence. The four to five times thicker portion underneath the water line is called the ridge keel (Timco & Burden, 1997), which determines the hydrodynamic interaction between ice and ocean (Castellani et al., 2014, 2015), and provides shelter to ice associated flora and fauna (Gradinger et al., 2010; Hop et al., 2000; Horner et al., 1992). Newly formed young ridges are a loose pile of individual ice blocks, characterized by significant macro-pore spaces in between the blocks (Strub-Klein & Sodom, 2012). This

© 2021. The Authors.

This is an open access article under the terms of the [Creative Commons Attribution License](https://creativecommons.org/licenses/by/4.0/), which permits use, distribution and reproduction in any medium, provided the original work is properly cited.

Writing – review & editing: Christian Katlein, Jean-Philippe Langelier, Alexandre Ouellet, Félix Lévesque-Desrosiers, Quentin Hisette, Benjamin A. Lange, Simon Lambert-Girard, Marcel Babin, Simon Thibault

complex geometry of blocks and cavities in a young ridge is very difficult to investigate, but it is exactly this complexity that gives rise to the unique and characteristic physical and biological processes associated with sea ice ridges. With time, thermodynamic processes cause the ridge to refreeze and consolidate in its inner part, while the edges of blocks melt into rounded shapes (Høyland, 2002). Thus, older ridges transform into more homogeneous, weathered, and thick ice bodies—also known as hummocks—over several years (Wadhams & Toberg, 2012).

According to diving observations, the complex internal geometry of pressure ridges provides shelter for all trophic levels of the ice associated ecosystem forming a biological hotspot (Assmy et al., 2013; Hop et al., 2000; Horner et al., 1992; Melnikov, 1997; Melnikov & Bondarchuk, 1987; Siegel et al., 1990). In addition to the ridges housing a particular microbial community (Ackley, 1986), small cavities provide physical protection from larger predators and ocean currents. Various algal communities thrive either hanging between ridge blocks (Lange, Flores, et al., 2017; Melnikov, 1997) or growing on the upward facing block sides (Fernández-Méndez et al.). On the leeward side of ridges, surface ice relative currents are much reduced, increasing the ability of phytoplankton and zooplankton to avoid being flushed away (Katlein et al., 2014). Smaller cavities provide shelter for fish such as the polar cod, while the bigger macro-pores also provide a home and hunting ground for seals (Furgal et al., 1996; Smith et al., 1991). Even polar bears seek shelter from the wind in between ridges and hunt for prey in ridge-associated seal lairs (Pilfold et al., 2014). Overall, pressure ridges are the most prominent and ubiquitous structuring element of the sea ice landscape which, despite their very dynamic evolution, are home to a condensed and highly productive form of the sea ice associated ecosystem. Due to their high complexity and generally lower light levels, they are however not explicitly included in most large-scale sea ice ecosystem models (Castellani et al., 2017), ignoring their ecological importance.

While sea ice thickness in the Arctic is declining (Haas et al., 2008; Kwok & Rothrock, 2009) and the ice pack has gotten more dynamic (Rampal et al., 2009), it is uncertain whether the role of sea ice ridges will become more or less important within the Arctic ecosystem. While the proportion of multiyear ice and thus of old ridges is likely to reduce (J. Maslanik et al., 2007; J.A Maslanik et al., 2011), younger—and thus more porous—ridges are likely to make up the Arctic ice pack in the future (Wadhams & Toberg, 2012). Investigations of physical properties, such as temperature, salinity, and strength of pressure ridges, have been conducted intensively, as the mechanical properties are of commercial interest to shipping and offshore operations (Leppäranta & Hakala, 1992; Richter-Menge & Cox, 1985; Strub-Klein & Sodom, 2012). Underwater investigations of ridges have only recently been aided by robotic vehicles (Fernández-Méndez et al.; Katlein et al., 2014; Lange, Flores, et al., 2017).

Light is one of the main drivers particularly of the autotrophic portion of the ice associated ecosystem, and it is very important to understand the nature and amount of light present within the ecological hotspots of ridge cavities. However, radiative transfer in such complex geometries cannot be investigated with the typical one-dimensional radiative transfer models, as they are only formulated for homogeneous slabs of ice (Katlein et al., 2016). Only few studies explicitly investigate the general decrease in light transmission due to the larger thickness of ridges (Lange et al., 2019; Lange, Katlein, et al., 2017) or try to parameterize it for model calculations (Fernández-Méndez et al.; Lange, Flores, et al., 2017). To improve habitat characterization and the representation of pressure ridges in ecological models, it is necessary to improve our understanding of radiative transfer in complex ridge geometries.

The objective of our work is to explicitly model the light field geometry within and underneath a typical young pressure ridge. As field data of the full internal geometry of a pressure ridge are not yet available, we use an artificial ridge generated in an ice mechanical model as input for a three-dimensional ray-tracing radiative transfer model. As this is not a representation of a real-world scenario, our main focus lies on understanding the radiative transfer processes governing the light field inside the ridge, and not the absolute value of light transmittance. Analysis of model output also allows for the comparison of existing and new parameterizations of radiative transfer through sea ice pressure ridges.

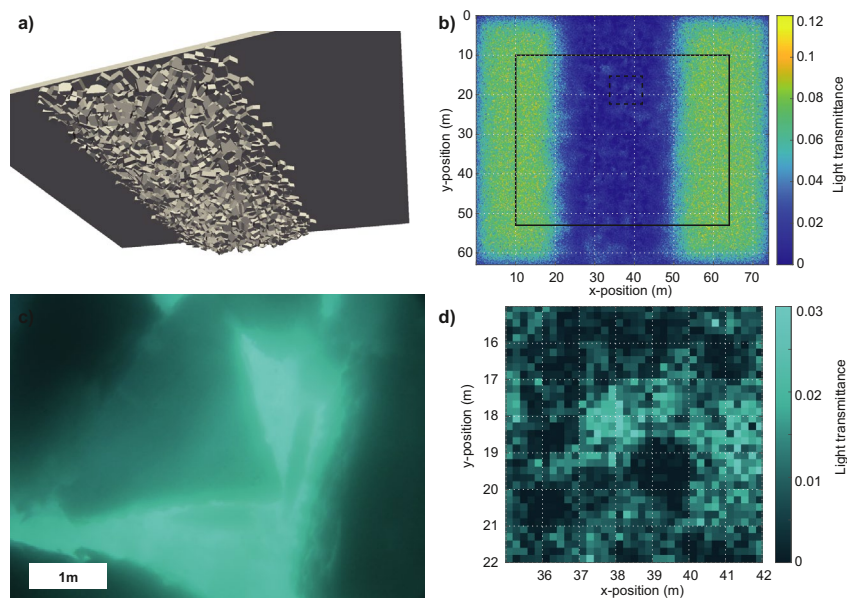


Figure 1. (a) Rendering of the investigated three-dimensional ridge geometry. (b) Downward planar irradiance field at 4 m depth as computed by the ray-tracing model. The black solid line rectangle depicts the area used for data analysis. (c) Upward looking photo taken by a remotely operated vehicle on August 19, 2018 during the AO18 expedition with the Swedish icebreaker Oden from ~ 10 m depth. (d) Close-up of the modeled irradiance field (dashed line rectangle in b) at a comparable spatial scale to the photograph in (c) with color bar adjusted to the picture colors. Individual ridge blocks are clearly discernible.

2. Materials and Methods

2.1. Sea Ice Model and the Investigated Ridge

There are plenty of available datasets from surface laser scanning and underwater multibeam sonar surveys, that can provide the full three-dimensional external geometry of pressure ridges (Melling et al., 1993; G. Williams et al., 2015; G.D. Williams et al., 2013). However, none of these studies provide insight into the internal structure of these complex ice geometries. Extensive drilling surveys (Høyland, 2002; Strub-Klein & Sudom, 2012) or geophysical methods, such as electromagnetic induction sounding (Hunkeler et al., 2016) and nuclear magnetic resonance (Nuber et al., 2017; Rabenstein et al., 2013) can provide some information on the internal ridge structure. The spatial resolution and contrast of these data are, however, not sufficient as input data for precise three-dimensional radiative transfer modeling.

To overcome this lack of data, we use an artificially created ridge geometry from a mechanical sea ice model used for simulating the interaction of sea ice with ships and structures (Hisette et al., 2017). In this model, a ridge is created using the “floating-up” technique, where buoyant ice blocks are released underneath a level ice sheet of 1 m thickness and afterward formed into a ridge of triangular cross section. The geometric size of the model domain (Figure 1b) is 74 by 63 m with a maximum ridge keel depth of 6.64 m. During the formation process, the ice blocks are pressed against each other so that a realistic ice-water porosity level is reached (An animation of this process can be found here: <https://www.youtube.com/watch?v=Zwn2J39E-OIA>). This creation mechanism results in a ridge without sail (Figure 1a), but the continuous ice sheet comes closer to a partly consolidated ridge than a simulation where ridge blocks are piled up by moving two ice sheets against each other. The ridge construction method has proved to produce realistic ridge geometries for ship-ice interaction modeling and ice tank testing (Hisette et al., 2017) and its geometric properties compare well to existing literature: The achieved macro-porosity of 35% and a ridge keel depth to keel width ratio around four is in line with ridge observations and the block length is in the correct relation to the sheet ice thickness (Strub-Klein & Sudom, 2012; Timco & Burden, 1997). Also the ratio of keel depth and block thickness fit previous observations and mechanical modeling (Parmerter & Coon, 1972). Of course, this ridge can only approximate a realistic situation, as many real processes, such as consolidation and snow accumulation are not taken into account.

2.2. Optical Model

The three-dimensional ridge geometry from the mechanical ice model was directly used in the optical design software Zemax Optic-Studio (Zemax LLC, Kirkland, USA). Ray tracing was performed with a total number of $5 \cdot 10^7$ rays using a diffuse lambertian light source representative of typical cloudy conditions in the summer sea ice area. We assigned homogenous optical properties to the ice resulting in broadband transmittance of 0.074 and albedo of 0.72 for the 1 m thick level ice sheet which is comparable to published literature values (Katlein et al., 2019, 2021; Light et al., 2008, 2015). The Lambertian light source emitted a realistic solar spectrum, and a database of measured real and imaginary refractive indices for ice was used (Warren & Brandt, 2008). The water was assumed to be free of scatterers, representing typical clear Arctic waters (Katlein et al., 2016; Pavlov et al., 2017; Taskjelle et al., 2017). The scattering coefficient of the ice was set to $\kappa_{si} = 200 \text{ m}^{-1}$ and we adopted a Henyey-Greenstein phase function with asymmetry parameter $g = 0.94$. For the real and imaginary refractive index of water we used the database “Water” built into Optic-Studio stock materials catalog MISC. Total scalar (E_0) and downwelling planar irradiances (E_d) were calculated at a spatial resolution of 0.2 by 0.2 m by the model at horizontal levels of 0, 1, 2, 3, 4, 5, and 6 m depth, both within the ice and in the underlying water. Downwelling planar irradiance E_d quantifies the energy flux across a horizontal area, and thus includes a cosine weighting of rays depending on zenith angle. Total scalar irradiance E_0 quantifies the energy flux through a point integrating equally weighted rays from all directions. We define the ratio $m = E_d / E_0$, which is similar to the mean cosine $\mu = E_{\text{net}} / E_0$ (Mobley, 1994) and is a rough index describing the geometric shape of the angular radiance distribution.

To overcome edge effects of the discrete ray tracing simulation, only the central part of the simulated ridge was used in the following evaluation (Figure 1b). The resulting light fields closely resemble upward looking images obtained from under-ice ROV dives (Figures 1c and 1d) showing that light field calculations of the ray tracing model generate realistic results.

2.3. Light Field Parameterizations

Most light transmittance parameterizations have been designed for level ice. Sea ice is often modeled as a plane parallel medium with homogenous material properties within one or several layers (Mobley et al., 1998; Perovich, 1990). Only simple parameterizations based on the exponential decay of light in a medium (Bouguer, 1729; Lambert, 1760) have been applied to the more complex situation for old ridges (Lange, Flores, et al., 2017) and young ridges (Fernández-Méndez et al.).

The first parameterization that, we evaluate in this study is the simple bulk-exponential approach. Light transmittance T is defined as the ratio of downwelling planar irradiance transmitted through the ice E_d divided by incoming downwelling planar irradiance at the ice surface E_i :

$$T = \frac{E_d}{E_i} \quad (1)$$

In its most simple form of a uniform slab of ice light transmittance can be parameterized as (Katlein et al., 2015; Lange, Flores, et al., 2017)

$$T = (1 - \alpha) \cdot \exp(-\kappa_{d,\text{ice}} \cdot z), \quad (2)$$

where α is the surface albedo and z is the total bulk ice thickness. In our model setup of level ice without vertically varying optical properties, the optical properties described in Section 2.2 yield a vertical attenuation coefficient for ice of $\kappa_{d,\text{ice}} = 1.33 \text{ m}^{-1}$.

For the more complex geometry of pressure ridges Fernández-Méndez et al. (2018) separated this formulation into a piecewise exponential plane parallel model, taking into account water pockets within the ice and several layers of ridge blocks. Adjusting their parameterization to our more idealized ridge results in

$$T = (1 - \alpha) \cdot \exp\left(-\kappa_{d,\text{ice}} \cdot (z_{\text{ice},1} + z_{\text{ice},2} + \dots) - \kappa_{d,w} \cdot (z_{w,1} + z_{w,2} + \dots)\right). \quad (3)$$

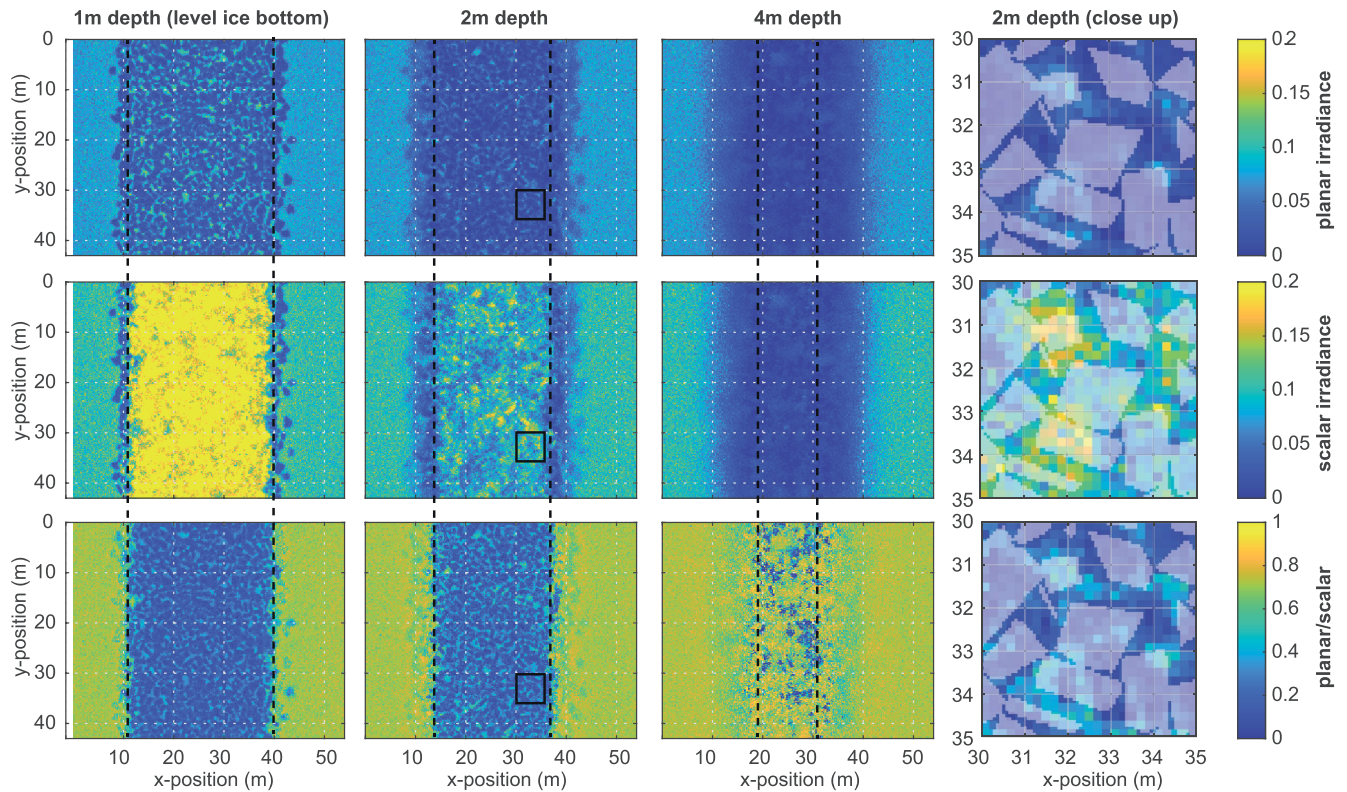


Figure 2. Horizontal slices of the calculated light field, within and underneath the ridge. Top row: Planar downwelling irradiance (normalized to ice surface) at the depths of 1, 2, and 4 m as well as a close up of the 2 m depth at a representative spot (black rectangles) within the ridge flank. Second row: Scalar irradiance. Third row: The ratio $m = E_d / E_0$ indicating the geometry of the light field. The area between the black dashed lines indicates the approximate region, where the horizontal slice lies within the ridge body.

Here $z_{ice,1} + z_{ice,2} + \dots = \sum_{i=1}^n z_{ice,i}$ describes the sum of ice thickness associated with n individual ridge blocks and $z_{w,1} + z_{w,2} + \dots$ the respective geometric thickness of water in the ridge voids. In the following, the first is referred to as the partial ice thickness, which can also be imagined as the amount of ice that would need to be drilled during a vertical ridge drilling exercise. While this formulation seems to explicitly account for a more realistic ice geometry, it clearly neglects laterally traveling light. Total bulk ice thickness z (including voids) and partial ice thickness were extracted from the simulated ridge geometry (described in Section 2.1) in all locations across the ridge. The average vertical attenuation coefficient in the water $\kappa_{d,w} = 0.02 \text{ m}^{-1}$ was determined from our simulation by fitting an exponential decay to the light field underneath level ice. The respective light transmittance was then calculated for each point using the above parameterization to allow for a comparison to the fully three-dimensional ray tracing model.

3. Results and Discussion

3.1. Calculated Light Field

The calculated light fields resulting from the ray-tracing calculations are shown in Figure 2. Apart from the slow decay of light with depth under level ice due to water absorption, the model also reproduces the general effect of lower light transmittance underneath the pressure ridge. Distinct shadows by individual ridge blocks are visible. These are also evident from upward looking ROV images providing validation to our model results (Figure 1c).

A main result from these calculations is that the scalar irradiance within the pressure ridge is considerably higher than at the same depth underneath level ice, particularly in the upper half of the ridge. This effect is caused by two factors. First, water filled cavities in the ridge lead to less total light attenuation. Second, the strong multiple scattering between ridge blocks changes the light field shape toward a more isotropic

radiance distribution. This increases particularly the total scalar irradiance versus downwelling planar irradiance (Figure 2), as evident by the decreased mean cosine (Section 3.2). Thus, light levels within ridge cavities are similarly high as within ridge blocks. These significantly higher light levels provide pelagic and ice associated algae and zooplankton with favorable light conditions within the ridge cavities. In their interior, ridges thus represent areas of higher light availability compared to the surroundings. In addition, macro pore space increases the habitable volume of the ridge offering also increased areas of ice surfaces as substrate. Only underneath, ridge keels shade the light field and decrease light transmittance. This particular light regime might further enhance positive factors such as the physical protection from currents and predators that the ridge associated ecosystem can benefit from (Gradinger et al., 2010).

3.2. Geometry of the Light Field in and Underneath the Ridge

Here, we use the ratio $m = E_d / E_0$ as a descriptor of the light field geometry. It describes the radiance distribution geometry between the two extreme cases of isotropic ($m = 0.25$) and unidirectional downwelling ($m = 1$) light fields. Values of $m < 0.25$ resemble a stronger upwelling portion of the light field caused by the upward-scattering of laterally traveling photons. Note, that this definition is different to the more common definition of the mean cosine of the downwelling light field as used in Matthes et al. (2019). It is, however, equivalent in the absence of upwelling light, for example, here under the level ice portion. As already mentioned above, multiple scattering within and in between ridge blocks bounces downwelling light back upwards within the ridge, while the low amount of scattering in the water column reduces upwelling light underneath ice. Organisms within the ridge thus receive similar amounts of light from all directions enhancing light availability for photosynthesis. Our model produces values of $m = 0.72$ comparable to the mean cosines shown by Matthes et al. (2019) for level ice (Figure 2). It also reproduces the known slow increase of the mean cosine with depth. Within the ridge, however, values are significantly lower. Values around $m = 0.1 - 0.3$ indicate an isotropic or directional in-ridge light field, where a majority of the light travels horizontally and not in downwelling direction. Inside the ridge, values increase from $m = 0.1 - 0.3$ inside the upper part of the ridge over $m = 0.2 - 0.4$ at the bottom of the ridge to $m = 0.7 - 0.8$ for regions below the ridge. Knowledge of these ratios enables derivation of scalar irradiance levels within ridges from the parameterizations of downwelling planar irradiances.

3.3. Comparison to Simple Ridge Models

Figure 3 evaluates the simple parameterizations of light transmission presented in Section 2.3. Transmittance parameterized on the basis of total ice thickness is expectedly lower than transmittance parameterized on the basis of partial ice thickness (Figure 3). Both parameterizations do not appropriately account for lateral smoothing of light transmittance pointing to the fact that estimations of the light field within a ridge from drill holes can both over- and underestimate the actual light intensity. This is caused by the strong variability of partial and total ice thickness along the ridge given by the chaotic block structure (Figure 4a).

Across ridge light profiles show a significant variability linked directly to local ridge block geometries (Figure 4b). Deviations are most prominent when ridge cavities of large vertical extent act as light guides through the ridge. While in our scenario we are able to evaluate local partial and total ice thickness in each spot, this will not be possible in a real setting, where ridge macroporosity data is acquired by ridge drilling. It is, however, evident that mean across-ridge light transmittance between raytracing and exponential models fit reasonably well. The parameterization using total ice thickness underestimates light transmittance, while the parameterization using partial ice thickness comes much closer to the average. Thus, parameterizations based on partial ice thickness will yield more realistic results. Both parameterizations fail to reproduce the light field at the outer ridge slopes, which are significantly smoother in the full three-dimensional simulation, than in the average parameterizations due to horizontal light propagation (Figure 4). For most large-scale models such inaccuracies would be acceptable, while more targeted modeling, for example, supporting in-situ sampling could suffer from undetected light field variability driven by specific local ridge geometry.

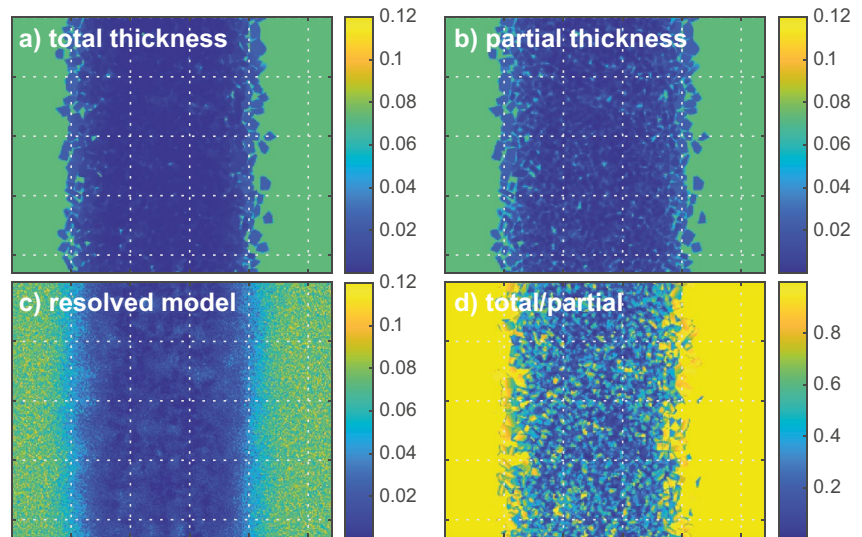


Figure 3. Light field at 5 m depth as parameterized based on total ice thickness (a), partial ice thickness (b), and derived from the fully resolved three-dimensional raytracing model (c). Panel (d) shows the ratio of the parameterizations based on total and partial sea ice thickness.

3.4. Potential Impact of the Ridge Sail and Consolidated Layer

In our model setup, the introduction of a simple idealized ridge sail did not show any significant effect. However, in reality a ridge sail may have additional influences on the light field within and under the ridge keel by influencing the distribution of snow around the sail, and/or the additional geometric effects and scattering of light within the surface ice blocks and air gaps of the sail. Snow distribution is largely controlled by the surface topography of the sea ice where snow is removed from high points (e.g., ridge sails and hummocks) and accumulates in low points or adjacent to high points (e.g., around ridge sails) (Lange et al., 2019; Sturm et al., 2002). This can result in thick snow accumulation around ridges, typically greater

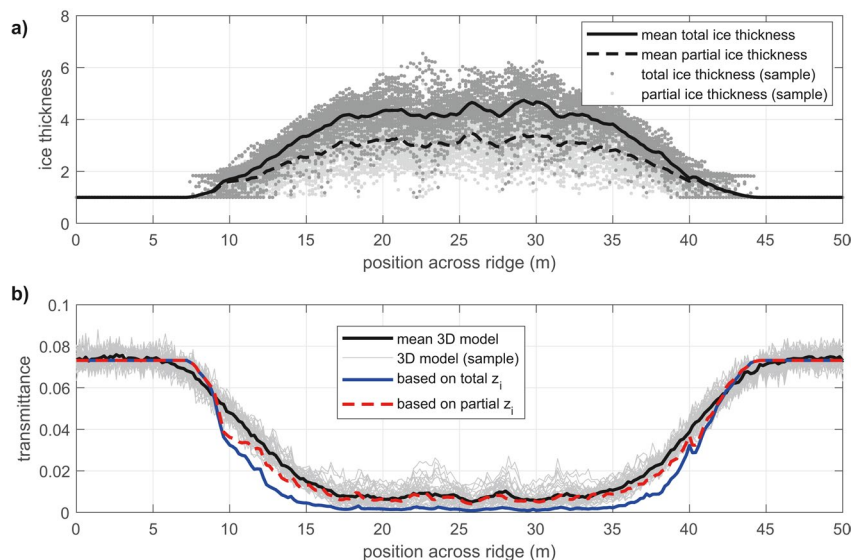


Figure 4. (a) Across-ridge profiles of mean total (solid line) and partial (dashed line) ice thickness. Light and dark gray dots represent individual pixels of partial and total ice thickness, respectively. (b) Across ridge planar irradiance profiles: Mean planar irradiance transmittance (solid black line) and individual profiles of planar irradiance transmittance at 5 m depth from raytracing (thin gray lines), and parameterized using partial (dashed blue line) and total ice thicknesses (solid blue line).

than 0.5 m, substantially reducing the absolute amount of light penetrating into the ridge from the top and further increasing the importance of both lateral light transfer and light guided through voids. This snow distribution is often asymmetrical due to prevailing wind directions, with more snow accumulating on the lee side of the ridge. The ridge sail, on the other hand, can have substantial regions of thin and snow-free ice protruding from the otherwise snow-covered ridge sail, which may have an opposite influence on the light field by locally increasing light penetration into the ridge. Also, the geometry of the surface blocks (i.e., angle relative to the solar inclination) may further increase light penetration into the ridge by decreasing the effective angle of sun inclination and minimizing specular reflection.

While the investigated ridge geometry somewhat mimics a thin consolidated layer, the amount of consolidation inside a ridge will certainly impact the light field. Consolidation will close voids that before acted as light guides, and will further reduce light transmission through the ridge by reducing its macro-porosity. This effect would be included in light estimates derived from light transmission parameterizations accounting for the macro-porosity of a ridge. These potential impacts and uncertainties should be included and assessed in future modeling studies and field measurements in order to quantify their respective effects.

4. Summary

We presented the first full three-dimensional modeling of the light field in a young pressure ridge. Model results are comparable to observations from upward looking under-ice cameras and thus are likely representative of a typical real-world situation. Light levels within ridge cavities are up to three times higher than in the surrounding waters, thus enhancing the ecological importance of pressure ridges for the sea ice system. The ridge light field is characterized by an isotropic or even upwelling radiance distribution with low values of the mean cosine. Particularly these presented ratios of planar and scalar irradiance inside the ridge will be of use when estimating light available for photosynthesis to convert between the different light field quantities. The high spatial variability of ridge block geometry can only be addressed correctly in a full ray tracing calculation, but simple parameterizations provide a reasonable mean estimate of both light transmittance and spatial variability. Parameterizations based on partial ice thickness yield more realistic results by accounting for macro-porosity of the ridge structure. It is also evident that such simple parameterizations cannot correctly reproduce the light field at the edge of ridges due to the importance of lateral light propagation.

The presented parameterizations are a simple way to estimate light levels inside a pressure ridge to ease habitat characterization and derive ridge associated photosynthetic production. Due to their simplicity, they can be used based on the results of traditional ridge drilling surveys, but also could be applied to large scale sea-ice ecosystem models.

The full internal structure of pressure ridges, as used for our study, is hard to acquire from field data. Further and more complex ray-tracing simulations of realistic scenarios of the light field in ridges could be based on the combined use of surface laser scanning, snow mapping and under-ice multibeam sonar mapping. This will require an indirect consideration of ridge internal geometry using measured macro-porosities from drilling data. Further simulations based on different ice mechanical ridge formation models could evaluate numerous scenarios tailored to specific observed ridge characteristics. When coupled with a snow-drift model, this might also allow some insight into the complex interplay of ridge sails and snow accumulation and their effect on the light field under and within the ridge. As fully resolved field data will likely not become available soon, the simple parameterizations considering average ridge macro-porosity derived here will allow for reasonable estimates of the light field around pressure ridges. This will aid both, in-situ habitat characterization, as well as large-scale modeling to provide realistic light fields to ridge.

Data Availability Statement

The modeled light fields are available at <https://doi.org/10.5281/zenodo.4491700> (Katlein & Langelier, 2021).

Acknowledgments

The writing of this manuscript was supported by a postdoctoral research fellowship to C. Katlein by Sentinel North supervised by Marcel Babin and Simon Thibault. The ROV work was funded by the Helmholtz Infrastructure Initiative "Frontiers in Arctic Marine Monitoring (FRAM)" and the Alfred-Wegener Institute. ROV observations during the AO18 expedition were supported by captain and crew of icebreaker Oden and the Swedish Polar Research Secretariat (SPRS). BAL is supported by funding from the Research Council of Norway projects: CAATEX (280531) and HAVOC (280292). The authors thank M. Hoppmann, P. Anhaus and M. Labaste for their help in conducting the ROV observations. Open access funding enabled and organized by Projekt DEAL.

References

- Ackley, S. (1986). Sea-ice pressure ridge microbial. *Antarctic Journal of the United States*, 21(5), 172.
- Assmy, P., Ehn, J. K., Fernández-Méndez, M., Hop, H., Katlein, C., Sundfjord, A., et al. (2013). Floating ice-algal aggregates below melting Arctic sea ice. *PLoS One*, 8(10), e76599. <https://doi.org/10.1371/journal.pone.0076599>
- Bouguer, P. (1729). *Essai d'Optique*. Claude Jombert.
- Castellani, G., Gerdes, R., Losch, M., & Lüpkes, C. (2015). Impact of sea-ice bottom topography on the Ekman pumping. In G. Lohmann, H. Meggers, V. Unnithan, D. Wolf-Gladrow, J. Notholt, & A. Bracher (Eds.), *Towards an interdisciplinary approach in earth system science: Advances of a Helmholtz graduate research school* (pp. 139–148). Springer International Publishing. https://doi.org/10.1007/978-3-319-13865-7_16
- Castellani, G., Losch, M., Lange, B. A., & Flores, H. (2017). Modeling Arctic sea-ice algae: Physical drivers of spatial distribution and algae phenology. *Journal of Geophysical Research: Oceans*, 122(9), 7466–7487. <https://doi.org/10.1002/2017jc012828>
- Castellani, G., Lüpkes, C., Hendricks, S., & Gerdes, R. (2014). Variability of Arctic sea-ice topography and its impact on the atmospheric surface drag. *Journal of Geophysical Research: Oceans*, 119(10), 6743–6762. <https://doi.org/10.1002/2013JC009712>
- Davis, N. R., & Wadhams, P. (1995). A statistical analysis of Arctic pressure ridge morphology. *Journal of Geophysical Research*, 100(C6), 10915–10925. <https://doi.org/10.1029/95jc00007>
- Fernández-Méndez, M., Olsen, L. M., Kauko, H. M., Meyer, A., Rösel, A., Merkouridi, I., et al. (2018). Algal hot spots in a changing Arctic ocean: Sea-ice ridges and the snow-ice interface. *Frontiers in Marine Science*, 5(75). <https://doi.org/10.3389/fmars.2018.00075>
- Furgal, C. M., Kovacs, K. M., & Innes, S. (1996). Characteristics of ringed seal, *Phoca hispida*, subnivean structures and breeding habitat and their effects on predation. *Canadian Journal of Zoology*, 74(5), 858–874. <https://doi.org/10.1139/z96-100>
- Gradinger, R., Bluhm, B., & Iken, K. (2010). Arctic sea-ice ridges—Safe heavens for sea-ice fauna during periods of extreme ice melt? *Deep Sea Research Part II: Topical Studies in Oceanography*, 57(1–2), 86–95. <https://doi.org/10.1016/j.dsr2.2009.08.008>
- Haas, C., Pfaffling, A., Hendricks, S., Rabenstein, L., Etienne, J.-L., & Rigor, I. (2008). Reduced ice thickness in Arctic Transpolar Drift favors rapid ice retreat. *Geophysical Research Letters*, 35(17), L17501. <https://doi.org/10.1029/2008gl034457>
- Hissette, Q., Alekseev, A., & Seidel, J. (2017). Discrete element simulation of ship breaking through ice ridges. In *The 27th International Ocean and Polar Engineering Conference* (p. 9). International Society of Offshore and Polar Engineers.
- Hop, H., Poltermann, M., Lønne, O. J., Falk-Petersen, S., Korsnes, R., & Budgell, W. P. (2000). Ice amphipod distribution relative to ice density and under-ice topography in the northern Barents Sea. *Polar Biology*, 23(5), 357–367. <https://doi.org/10.1007/s003000050456>
- Horner, R., Ackley, S. F., Dieckmann, G. S., Gulliksen, B., Hoshiai, T., Legendre, L., et al. (1992). Ecology of sea ice biota. 1. Habitat, terminology, and methodology. *Polar Biology*, 12(3–4), 417–427. <https://doi.org/10.1007/bf00243113>
- Høyland, K. V. (2002). Consolidation of first-year sea ice ridges. *Journal of Geophysical Research*, 107(C6), 15-11–15-16. <https://doi.org/10.1029/2000jc000526>
- Hunkeler, P. A., Hoppmann, M., Hendricks, S., Kalscheuer, T., & Gerdes, R. (2016). A glimpse beneath Antarctic sea ice: Platelet layer volume from multifrequency electromagnetic induction sounding. *Geophysical Research Letters*, 43(1), 222–231. <https://doi.org/10.1002/2015gl065074>
- Katlein, C., Arndt, S., Belter, H. J., Castellani, G., & Nicolaus, M. (2019). Seasonal evolution of light transmission distributions through arctic sea ice. *Journal of Geophysical Research: Oceans*, 124, 5418, 5435. <https://doi.org/10.1029/2018JC014833>
- Katlein, C., Arndt, S., Nicolaus, M., Perovich, D. K., Jakuba, M. V., Suman, S., et al. (2015). Influence of ice thickness and surface properties on light transmission through Arctic sea ice. *Journal of Geophysical Research: Oceans*, 120(9), 5932–5944. <https://doi.org/10.1002/2015JC010914>
- Katlein, C., Fernández-Méndez, M., Wenzhöfer, F., & Nicolaus, M. (2014). Distribution of algal aggregates under summer sea ice in the Central Arctic. *Polar Biology*, 38, 719–731. <https://doi.org/10.1007/s00300-014-1634-3>
- Katlein, C., & Langelier, J.-P. (2021). *Computed light fields within a sea ice pressure ridge*. Zenodo. <https://doi.org/10.5281/zenodo.4491701>
- Katlein, C., Perovich, D. K., & Nicolaus, M. (2016). Geometric effects of an inhomogeneous sea ice cover on the under ice light field. *Frontiers of Earth Science*, 4, 1–10. <https://doi.org/10.3389/feart.2016.00006>
- Katlein, C., Valcic, L., Lambert-Girard, S., & Hoppmann, M. (2021). New insights into radiative transfer within sea ice derived from autonomous optical propagation measurements. *The Cryosphere*, 15(1), 183–198. <https://doi.org/10.5194/tc-15-183-2021>
- Kwok, R., & Rothrock, D. A. (2009). Decline in Arctic sea ice thickness from submarine and ICESat records: 1958–2008. *Geophysical Research Letters*, 36. <https://doi.org/10.1029/2009gl039035>
- Lambert, J. H. (1760). *Photometria*.
- Lange, B. A., Flores, H., Michel, C., Beckers, J. F., Bublit, A., Casey, J. A., et al. (2017). Pan-Arctic sea ice-algal chl *a* biomass and suitable habitat are largely underestimated for multiyear ice. *Global Change Biology*, 23(11), 4581–4597. <https://doi.org/10.1111/gcb.13742>
- Lange, B. A., Haas, C., Charette, J., Katlein, C., Campbell, K., Duerksen, S., et al. (2019). Contrasting ice algae and snow-dependent irradiance relationships between first-year and multiyear sea ice. *Geophysical Research Letters*, 46(19), 10834–10843. <https://doi.org/10.1029/2019gl082873>
- Lange, B. A., Katlein, C., Castellani, G., Fernández-Méndez, M., Nicolaus, M., Peeken, I., & Flores, H. (2017). Characterizing spatial variability of ice algal chlorophyll *a* and net primary production between sea ice habitats using horizontal profiling platforms. *Frontiers in Marine Science*, 4(349). <https://doi.org/10.3389/fmars.2017.00349>
- Leppäranta, M., & Hakala, R. (1992). The structure and strength of first-year ice ridges in the Baltic Sea. *Cold Regions Science and Technology*, 20(3), 295–311. [https://doi.org/10.1016/0165-232X\(92\)90036-T](https://doi.org/10.1016/0165-232X(92)90036-T)
- Light, B., Grenfell, T. C., & Perovich, D. K. (2008). Transmission and absorption of solar radiation by Arctic sea ice during the melt season. *Journal of Geophysical Research*, 113(C3). <https://doi.org/10.1029/2006jc003977>
- Light, B., Perovich, D. K., Webster, M. A., Polashenski, C., & Dadic, R. (2015). Optical properties of melting first-year Arctic sea ice. *Journal of Geophysical Research: Oceans*, 120(11), 7657–7675. <https://doi.org/10.1002/2015JC011163>
- Maslanik, J. A., Fowler, C., Stroeve, J., Drobot, S., Zwally, J., Yi, D., & Emery, W. (2007). A younger, thinner Arctic ice cover: Increased potential for rapid, extensive sea-ice loss. *Geophysical Research Letters*, 34(24), L24501. <https://doi.org/10.1029/2007gl032043>
- Maslanik, J., Stroeve, J., Fowler, C., & Emery, W. (2011). Distribution and trends in Arctic sea ice age through spring 2011. *Geophysical Research Letters*, 38. <https://doi.org/10.1029/2011gl047735>
- Massicotte, P., Peeken, I., Katlein, C., Flores, H., Huot, Y., Castellani, G., et al. (2019). Sensitivity of phytoplankton primary production estimates to available irradiance under heterogeneous sea ice conditions. *Journal of Geophysical Research: Oceans*, 124(8), 5436–5450. <https://doi.org/10.1029/2019jc015007>

- Matthes, L. C., Ehn, J. K., Girard, S.-L., Pogorzelec, N. M., Babin, M., & Mundy, C. J. (2019). Average cosine coefficient and spectral distribution of the light field under sea ice: Implications for primary production. *Elementa: Science of the Anthropocene*, 7(1). <https://doi.org/10.1525/elementa.363>
- Meier, W. N., Hovelsrud, G. K., van Oort, B. E. H., Key, J. R., Kovacs, K. M., Michel, C., et al. (2014). Arctic sea ice in transformation: A review of recent observed changes and impacts on biology and human activity. *Reviews of Geophysics*, 52(3), 185–217. <https://doi.org/10.1002/2013rg000431>
- Melling, H., Topham, D. R., & Riedel, D. (1993). Topography of the upper and lower surfaces of 10 hectares of deformed sea ice. *Cold Regions Science and Technology*, 21(4), 349–369. [https://doi.org/10.1016/0165-232X\(93\)90012-W](https://doi.org/10.1016/0165-232X(93)90012-W)
- Melnikov, I. A. (1997). *The Arctic sea ice ecosystem*. Cambridge University Press.
- Melnikov, I. A., & Bondarchuk, L. L. (1987). To the ecology of the mass aggregations of colonial diatom algae under the Arctic drifting sea ice. *Okeanologiya*, 27(2), 317–321.
- Mobley, C. D. (1994). *Light and water: Radiative transfer in natural waters*. Academic Press.
- Mobley, C. D., Cota, G. F., Grenfell, T. C., Maffione, R. A., Pegau, W. S., & Perovich, D. K. (1998). Modeling light propagation in sea ice. *IEEE Transactions on Geoscience and Remote Sensing*, 36(5), 1743–1749. <https://doi.org/10.1109/36.718642>
- Nicolaus, M., Katlein, C., Maslanik, J., & Hendricks, S. (2012). Changes in Arctic sea ice result in increasing light transmittance and absorption. *Geophysical Research Letters*, 39, L24501. <https://doi.org/10.1029/2012gl053738>
- Nuber, A., Rabenstein, L., Lehmann-Horn, J. A., Hertrich, M., Hendricks, S., Mahoney, A., & Eicken, H. (2017). Water content estimates of a first-year sea-ice pressure ridge keel from surface-nuclear magnetic resonance tomography. *Annals of Glaciology*, 54(64), 33–43. <https://doi.org/10.3189/2013AoG64A205>
- Parmeter, R. R., & Coon, M. D. (1972). Model of pressure ridge formation in sea ice. *Journal of Geophysical Research*, 77(33), 6565–6575. <https://doi.org/10.1029/JC077i033p06565>
- Pavlov, A. K., Taskjelle, T., Kauko, H. M., Hamre, B., Hudson, S. R., Assmy, P., et al. (2017). Altered inherent optical properties and estimates of the underwater light field during an Arctic under-ice bloom of *Phaeocystis pouchetii*. *Journal of Geophysical Research: Oceans*, 122(6), 4939–4961. <https://doi.org/10.1002/2016JC012471>
- Perovich, D. K. (1990). Theoretical estimates of light reflection and transmission by spatially complex and temporally varying sea ice covers. *Journal of Geophysical Research*, 95(C6), 9557–9567. <https://doi.org/10.1029/JC095iC06p09557>
- Pilfold, N. W., Derocher, A. E., Stirling, I., & Richardson, E. (2014). Polar bear predatory behavior reveals seascape distribution of ringed seal lairs. *Population Ecology*, 56(1), 129–138. <https://doi.org/10.1007/s10144-013-0396-z>
- Rabenstein, L., Nuber, A., Lehmann-Horn, J. A., Hertrich, M., Hendricks, S., Mahoney, A. R., & Eicken, H. (2013). Porosity of a sea-ice pressure ridge keel estimated on the basis of surface nuclear magnetic resonance measurements. In *Cryosphere geophysics: Understanding a changing climate with subsurface imaging*.
- Rampal, P., Weiss, J., & Marsan, D. (2009). Positive trend in the mean speed and deformation rate of Arctic sea ice, 1979–2007. *Journal of Geophysical Research*, 114(C5), C05013. <https://doi.org/10.1029/2008JC005066>
- Richter-Menge, J. A., & Cox, G. F. N. (1985). Structure, salinity and density of multi-year sea ice pressure ridges. *Journal of Energy Resources Technology*, 107(4), 493–497. <https://doi.org/10.1115/1.3231224>
- Siegel, V., Bergström, B., Strömberg, J. O., & Schalk, P. H. (1990). Distribution, size frequencies and maturity stages of krill, *Euphausia superba*, in relation to sea-ice in the Northern Weddell Sea. *Polar Biology*, 10(7), 549–557. <https://doi.org/10.1007/BF00233705>
- Smith, T. G., Hammill, M. O., & Taugbøl, G. (1991). A review of the developmental, behavioral and physiological adaptations of the ringed seal, *Phoca hispida*, to life in the Arctic winter. *Arctic*, 44(2), 124–131. <https://doi.org/10.14430/arctic1528>
- Strub-Klein, L., & Sudom, D. (2012). A comprehensive analysis of the morphology of first-year sea ice ridges. *Cold Regions Science and Technology*, 82, 94–109. <https://doi.org/10.1016/j.coldregions.2012.05.014>
- Sturm, M., Holmgren, J., & Perovich, D. K. (2002). Winter snow cover on the sea ice of the Arctic ocean at the surface heat budget of the Arctic ocean (SHEBA): Temporal evolution and spatial variability. *Journal of Geophysical Research*, 107(C10). <https://doi.org/10.1029/2000JC000400>
- Taskjelle, T., Granskog, M. A., Pavlov, A. K., Hudson, S. R., & Hamre, B. (2017). Effects of an Arctic under-ice bloom on solar radiant heating of the water column. *Journal of Geophysical Research: Oceans*, 122(1), 126–138. <https://doi.org/10.1002/2016JC012187>
- Timco, G. W., & Burden, R. P. (1997). An analysis of the shapes of sea ice ridges. *Cold Regions Science and Technology*, 25(1), 65–77. [https://doi.org/10.1016/S0165-232X\(96\)00017-1](https://doi.org/10.1016/S0165-232X(96)00017-1)
- Wadhams, P., & Toberg, N. (2012). Changing characteristics of arctic pressure ridges. *Polar Science*, 6(1), 71–77. <https://doi.org/10.1016/j.polar.2012.03.002>
- Warren, S. G., & Brandt, R. E. (2008). Optical constants of ice from the ultraviolet to the microwave: A revised compilation. *Journal of Geophysical Research*, 113(D14). <https://doi.org/10.1029/2007JD009744>
- Williams, G., Maksym, T., Wilkinson, J., Kunz, C., Murphy, C., Kimball, P., & Singh, H. (2015). Thick and deformed Antarctic sea ice mapped with autonomous underwater vehicles. *Nature Geoscience*, 8(1), 61–67. <https://doi.org/10.1038/ngeo2299>
- Williams, G. D., Maksym, T., Kunz, C., Kimball, P., Singh, H., Wilkinson, J., et al. (2013). Beyond point measurements: Sea ice floes characterized in 3-D. *Eos, Transactions American Geophysical Union*, 94(7), 69–70. <https://doi.org/10.1002/2013EO070002>